A Hierarchical Modeling for Reactive Power Optimization With Joint Transmission and Distribution Networks by Curve Fitting

Ding, Tao; Li, Cheng; Huang, Can; Yang, Yongheng; Li, Fangxing; Blaabjerg, Frede

Published in:
IEEE Systems Journal

DOI (link to publication from Publisher):
10.1109/JSYST.2016.2642218

Publication date:
2018

Document Version
Accepted author manuscript, peer reviewed version

This article has been accepted for inclusion in a future issue of this journal. Content is final as presented, with the exception of pagination.

A Hierarchical Modeling for Reactive Power Optimization With Joint Transmission and Distribution Networks by Curve Fitting

Tao Ding, *Member, IEEE*, Cheng Li, *Student Member, IEEE*, Can Huang, *Member, IEEE*, Yongheng Yang, *Member, IEEE*, Fangxing Li, *Fellow, IEEE*, and Frede Blaabjerg, *Fellow, IEEE*

***Abstract*—In order to solve the reactive power optimization with joint transmission and distribution networks, a hierarchical modeling method is proposed in this paper. It allows the reactive power optimization of transmission and distribution networks to be performed separately, leading to a master–slave structure and improves traditional centralized modeling methods by alleviating the big data problem in a control center. Specifically, the transmission-distribution-network coordination issue of the hierarchical modeling method is investigated. First, a curve-fitting approach is developed to provide a cost function of the slave model for the master model, which reflects the impacts of each slave model. Second, the transmission and distribution networks are decoupled at feeder buses, and all the distribution networks are coordinated by the master reactive power optimization model to achieve the global optimality. Numerical results on two test systems verify the effectiveness of the proposed hierarchical modeling and curve-fitting methods.**

***Index Terms*—Curve fitting, decomposition, hierarchical modeling, joint networks, reactive power optimization.**

I. Introduction

REACTIVE power optimization, employed in power system operation, normally aims to minimize the total transmission losses under a given load level by determining all controllable variables (e.g., reactive power compensators, reactive power outputs of generators, tap ratios of transformers, and outputs of shunt capacitors or reactors) while satisfying various system design and operational requirements [1]. It is normally conducted by the automatic voltage control in every time interval of several minutes (as in 15–60 min) to provide the voltage set points for pivot buses and the remote control signals for the reactors, shunt capacitors, and tap ratios of transformers, respectively [2], [3].

Conventionally, the reactive power optimization problem can be formulated as a mixed-integer nonlinear programming (MINLP) model and be further solved by two categories of approaches [4]. One is the intelligent approach, including simulated annealing [5], two-layer simulated annealing [6], evolutionary algorithms [7], [8], fuzzy clustering [9]–[11], genetic algorithms [12], tabu search [13], particle swarm optimization methods [14], [15], seeker optimization algorithms [16], etc. The other one is the conventional approach, such as gradient-based optimization algorithms [17], quadratic programming [18], successive linear programming [19], successive quadratic programming [20], the Newton method [21], interior-point (IP) methods [22], mixed-integer programming [23], and some decomposition methods [24].

Today, many countries, such as China, use the centralized power network modeling. The energy management system (EMS) of a control center collects a large amount of information from every distribution network and sends exact operation and control signals to the subordinated distribution management systems (DMS). In this way, the models of transmission and distribution networks can be merged into one complete model. The advantage of centralized modeling is that it can provide the exact global optimal solution. However, using this centralized modeling method in large-scale power grids will result in several problems.

1) Highly reliable and heavy communications are required to set up a complete model.
2) Huge numbers of data will come into the control center to form a complete mode—big data issues, delays in model updating, and sufficient disaster recovery backup should, thus, be taken into consideration.
3) In some special cases, the detailed models of subordinated distribution networks are private, and only limited information can be provided to the control center.

In order to tackle the above issues, an organizational structure of a power system operation in China has deployed a multi-

Manuscript received July 28, 2016; revised October 29, 2016; accepted December 7, 2016. This work was supported in part by the National Key Research and Development Program of China (2016YFB0901904), in part by the National Natural Science Foundation of China under Grant 51607137, in part by the China Postdoctoral Science Foundation (2015M580847), in part by the Natural Science Basis Research Plan in Shaanxi Province of China (2016JQ5015), in part by the Project of the State Key Laboratory of Electrical Insulation, and in part by the Power Equipment in Xi'an Jiaotong University (EIPE16301). This work was performed under the auspices of the U.S. Department of Energy by Lawrence Livermore National Laboratory under Contract DE-AC52-07NA27344 with Release Number LLNL-JRNL-716920.

T. Ding and C. Li are with the State Key Laboratory of Electrical Insulation and Power Equipment, School of Electrical Engineering, Xi'an Jiaotong University, Xi'an 710049, China (e-mail: tding15@mail.xjtu.edu.cn; jackcleebest@hotmail.com).

C. Huang is with the Lawrence Livermore National Laboratory, Livermore, CA 94550 USA (e-mail: can7huang@gmail.com).

Y. Yang and F. Blaabjerg are with the Department of Energy Technology, Aalborg University, Aalborg DK-9220, Denmark (e-mail: yoy@et.aau.dk; fbl@et.aau.dk).

F. Li is with the Department of Electrical Engineering and Computer Science, The University of Tennessee, Knoxville, TN 37996 USA (e-mail: fli6@utk.edu).

Digital Object Identifier 10.1109/JSYST.2016.2642218

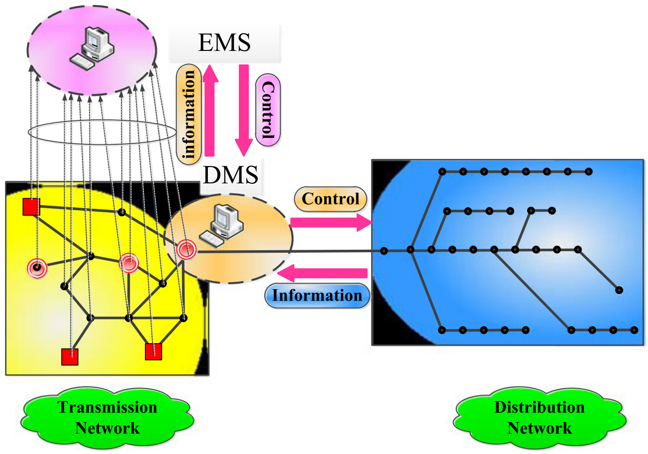

Fig. 1. Example of joint transmission and distribution networks.

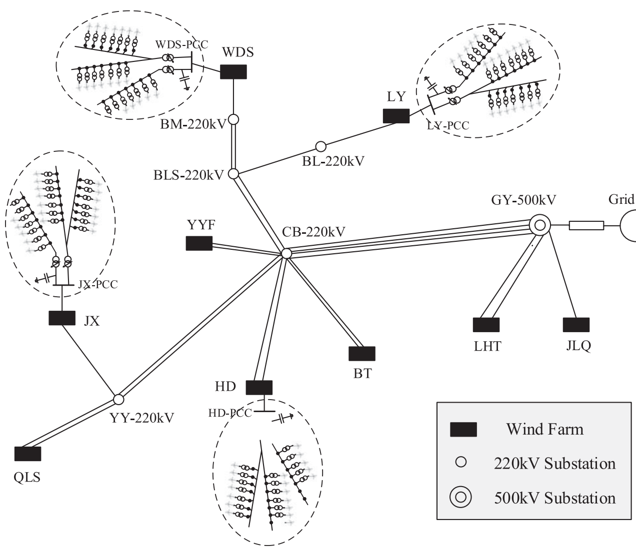

Fig. 2. Hierarchical model of wind resources in Northern China.

level pattern in recent years, as shown in Fig. 1 [25], [26]. The models of transmission and distribution networks are hierarchically administrated; they have demonstrated advances over the centralized ones and led to a master–slave control and dispatch structure.

For the slave level (the distribution network), a monitoring system is installed in each individual DMS that has its own administration privilege and only aggregates the detailed local information within its administrating distribution network. Then, the optimal decision is performed based on the obtained local information.

For the master level (the transmission network), the EMS receives the information from each DMS, according to the IEC 61850 standard, and preforms a global optimal decision to coordinate multiple DMS. However, it should be noted that only limited information, instead of detailed information, is allowed to be exchanged, which aims to alleviate the possibility of a huge amount of data from subordinated systems.

In addition, this hierarchical modeling method has been used in most centralized integrated wind farms in China, as shown in Fig. 2. In China, the wind energy resources are mainly distributed in the northern and northwestern areas, which are far from the major load centers in the eastern and coastal areas [25]. At the wind-farm-side level, the topology and all wind units can be explicitly modeled in each wind farm, and many wind units are distributed and connected to the same 35-kV level bus of 35-kV/220-kV substations, called the point-of-common coupling (PCC) buses. At the system-wide level, some large-scale wind farms are connected to the high-voltage substation (e.g., 220–500 kV). Here, detailed information of each wind farm (e.g., detailed states of wind units and topologies of each wind farm) cannot be provided to the control center since the data are private; instead, only limited information is allowed to be exchanged, such as the total power and voltage magnitude of the PCC bus.

The hierarchical modeling has a unique challenge: the modeling of reactive power optimization for distribution and transmission networks is established separately, but the optimal decisions are strongly coupled. If the decisions of the hierarchical systems are optimized separately, the global optimality will be sacrificed due to the lack of coordination.

Recently, there have been many papers proposed to discuss the topic of coordinated transmission and distribution network optimization. In [27] and [28], the heterogeneous decentralized algorithm was proposed to study the economic dispatch problem, which is in fact a convex optimization problem, meaning the heterogeneous method can give the global optimization solution. Li *et al.* [29] focused on the nonconvex optimization problem for hybrid transmission and distribution networks, but the heterogeneous algorithm may only lead to a local optimal. Moreover, the heterogeneous algorithm is an iteration method that needs the coordination message between transmission and distribution networks, which itself needs highly reliable heavy communications. Lin *et al.* [30] adopted a generalized Benders decomposition method to solve the reactive power optimization model considering transmission and distribution networks. However, this method requires the subproblems to be convex so that the Benders cut is a valid cut. In reality, the shunt capacitors/reactors are discrete control variables in the reactive power optimization, challenging the Benders decomposition method. Ref. [31] discussed the dynamic simulations for coordinating the transmission and distribution networks.

In this paper, a curve-fitting approach is proposed for the mixed-integer programming problems to provide a cost function of each slave-level model for the master model; this approach reflects the impact of slave-level models on the feeder buses. Furthermore, the modeling of feeder buses for the master model is replaced by the calculated cost functions such that the transmission and distribution networks are decoupled at the feeder buses/substations. Thus, the distribution networks can be coordinated by the master-level reactive power optimization model. In particular, the proposed method is a direct method based on the curve-fitting approach and does not need the coordination message, alleviating the pressure on the communication systems.

The contributions of this paper are summarized as follows.

1) A hierarchical modeling for reactive power optimization with joint transmission and distribution networks is proposed to alleviate a huge amount of data for the control center, in contrast to the centralized modeling.

2) A decomposition method is utilized for the joint reactive power optimization model by the curve-fitting approach, which decouples the transmission and distribution networks.

The rest of this paper is organized as follows. In Section II, a sequential IP method is presented to solve the general reactive power optimization model. In Section III, a curve-fitting function (CFF) is proposed to decompose the reactive power optimization model with joint transmission and distribution networks. Following, in Section IV, numerical results on two test systems and comparison with the centralized approach demonstrate the effectiveness of the proposed method. Finally, conclusions are drawn in Section V.

II. Formulation of Reactive Power Optimization

In general, the reactive power optimization problem to minimize transmission losses can be written as

$$\min \sum_{(i,j)\in \mathrm{Edge}} \left(r_{ij} I_{ij}^2\right) \tag{1-a}$$

$$\text{s.t.}\ \ P_i = U_i \sum_{(i,j)\in \mathrm{Edge}} U_j \left(G_{ij}\cos\theta_{ij} + B_{ij}\sin\theta_{ij}\right) \quad \forall i \in \mathrm{Node} \tag{1-b}$$

$$Q_i + Q_{c,i} = U_i \sum_{(i,j)\in \mathrm{Edge}} U_j \left(G_{ij}\sin\theta_{ij} - B_{ij}\cos\theta_{ij}\right) \quad \forall i \in \mathrm{Node} \tag{1-c}$$

$$U_i^{\min} \le U_i \le U_i^{\max} \quad \forall i \in \mathrm{Node} \tag{1-d}$$

$$I_{ij} \le I_{ij}^{\max} \quad \forall (i,j) \in \mathrm{Edge} \tag{1-e}$$

$$Q_{c,j}^{\min} \le Q_{c,j} \le Q_{c,j}^{\max} \quad \forall j \in \Omega \tag{1-f}$$

$$Q_{c,j} \in \textbf{integers} \quad \forall j \in \Omega \cap \Omega_D \tag{1-g}$$

$$I_{ij} = \frac{U_i^2 + U_j^2 - 2U_iU_j\cos\theta_{ij}}{r_{ij}^2 + x_{ij}^2} \quad \forall (i,j) \in \mathrm{Edge} \tag{1-h}$$

where Node is the set of buses and Edge is the set of branches; (*i*, *j*) is a branch whose "from" bus is *i* and "to" bus is *j*; r_{ij} and x_{ij} are the resistance and reactance of branch (*i*, *j*); G_{ij} and B_{ij} are the real and imaginary parts of the element in the bus admittance matrix; U_i, P_i, and Q_i denote the voltage magnitude, injected active power, and injected reactive power at bus *i*; θ_{ij} is the voltage angle difference between bus *i* and bus *j*; $Q_{c,j}$ is the reactive power compensation at bus *j*; $Q_{c,j}^{\max}$ and $Q_{c,j}^{\min}$ are the upper and lower bound of the reactive power compensation at bus *j*; Ω is the set of buses at which the reactive power compensators are installed; $\Omega_D \subseteq \Omega$ denotes the set of buses that possess discrete shunt capacitors/reactors; $U_i^{\max}$ and $U_i^{\min}$ are the upper and lower bound of voltage magnitude at bus *i*; and $I_l^{\max}$ is the current capacity limit of the branch (*i*, *j*).

The reactive power optimization problem (1) can be compactly formulated as a mixed-integer programming problem

$$\min\ f\left(\boldsymbol{x}_1, \boldsymbol{x}_2, \boldsymbol{x}_3\right) \tag{2-a}$$

$$\text{s.t.}\ \ \boldsymbol{g}\left(\boldsymbol{x}_1, \boldsymbol{x}_2, \boldsymbol{x}_3\right) = \boldsymbol{0} \tag{2-b}$$

$$\boldsymbol{x}_1^{\min} \le \boldsymbol{x}_1 \le \boldsymbol{x}_1^{\max} \tag{2-c}$$

$$\boldsymbol{x}_2^{\min} \le \boldsymbol{x}_2 \le \boldsymbol{x}_2^{\max} \tag{2-d}$$

$$\boldsymbol{x}_3^{\min} \le \boldsymbol{x}_3 \le \boldsymbol{x}_3^{\max} \tag{2-e}$$

where $f(\cdot)$ is the total transmission losses; $\boldsymbol{g}(\cdot)$ is the power flow equations; $\boldsymbol{x}_1 = [\boldsymbol{Q}_{\mathrm{C}}, \boldsymbol{T}]^T$ are discrete control variables including shunt capacitors/reactors and transformer tap ratios; $\boldsymbol{x}_2 = [\boldsymbol{Q}_{\mathrm{G}}]^T$ are continuous control variables including reactive power outputs of generators or static voltage generators; $\boldsymbol{x}_3 = [\boldsymbol{P}_G, \boldsymbol{\theta}, \boldsymbol{U}]^T$ are continuous state variables including active power output of slack buses, voltage angles, and magnitudes of each bus; and $(\boldsymbol{x}_1^{\min}, x_2^{\min}, x_3^{\min})$ and $(\boldsymbol{x}_1^{\max}, x_2^{\max}, x_3^{\max})$ denote the lower and upper bound of each variable.

Each discrete integer variable can be expressed as

$$x_{1,i} = y_i \cdot \mathrm{step}_i + x_{1,i}^{\min}, \quad i = 1, 2, ..., l \tag{3}$$

where *l* is the number of discrete variables; step_i is the step size of discrete variables $x_{1,i}$, and y_i is an integer number which can be equivalent to a combination of the 0-1 binary auxiliary variables $y_{i,0}, y_{i,1}, ..., y_{i,t_i}$, such that

$$x_{1,i} = x_{1,i}^{\min} + \mathrm{step}_i\left(2^0 y_{i,0} + 2^1 y_{i,1} + ... + 2^{t_i} y_{i,t_i}\right) \tag{4}$$

where t_i is an integer number that is determined by

$$\log_2\left(\frac{x_{1,i}^{\max} - x_{1,i}^{\min}}{\mathrm{step}_i} + 1\right) - 1 \le t_j \le \log_2\left(\frac{x_{1,i}^{\max} - x_{1,i}^{\min}}{\mathrm{step}_i} + 1\right). \tag{5}$$

When using (3)–(5), problem (2) can be transformed into the following general MINLP problem:

$$\min\ f\left(\boldsymbol{x}, \boldsymbol{y}\right) \tag{6-a}$$

$$\text{s.t.}\ \ \boldsymbol{g}\left(\boldsymbol{x}, \boldsymbol{y}\right) = \boldsymbol{0} \tag{6-b}$$

$$\boldsymbol{x}^{\min} \le \boldsymbol{x} \le \boldsymbol{x}^{\max} \tag{6-c}$$

where $\boldsymbol{y} \in \{0,1\}^m$ denotes the vector of discrete variables and $\boldsymbol{x} = [\boldsymbol{x}_2, \boldsymbol{x}_3]^T \in R^n$ denotes the vector of continuous variables subject to lower bound $\boldsymbol{x}^{\min}$ and upper bound $\boldsymbol{x}^{\max}$.

In general, the mixed-integer programming problem can be solved by various methods like the branch and bound [32] and the cutting plane [33]. The key to these methods is to relax the integer variables into continuous ones and solve the relaxed model to generate a lower bound. Hence, the relaxed model is expected to be at least a convex problem such that its global optimal solution can be guaranteed by the Karush–Kuhn–Tucker conditions. This kind of problem is called a mixed-integer convex programing problem.

Unfortunately, the MINLP in (6) is not a mixed-integer convex programming problem due to nonconvex power flow equations. This condition means that even after relaxing the integer

TABLE I
PROCEDURE OF THE SEQUENTIAL IP METHOD

Algorithm: Sequential Interior-Point Method for MINLP

Step 1: Select large enough values for the constants C and C^d;

Step 2: Solve the relaxed problem:

$$\min \quad f(\boldsymbol{x}, \boldsymbol{y}) \tag{7-a}$$
$$\text{s.t.} \quad \boldsymbol{g}(\boldsymbol{x}, \boldsymbol{y})=\boldsymbol{0} \tag{7-b}$$
$$0 \le y_i \le 1, \quad i=1,2,\ldots,m \tag{7-c}$$
$$\boldsymbol{x}^{\min} \le \boldsymbol{x} \le \boldsymbol{x}^{\max} \tag{7-d}$$
$$f(\boldsymbol{x}, \boldsymbol{y}) \le C-\varepsilon \tag{7-e}$$

Step 3: Let $(\boldsymbol{x}^*, \boldsymbol{y}^*)$ denote one local optimal solution of (7);

Step 4: Use $(\boldsymbol{x}^*, \boldsymbol{y}^*)$ to initialize the IP algorithm and solve the sub-problem:

$$\min \quad f(\boldsymbol{x}, \boldsymbol{y}) \tag{8-a}$$
$$\text{s.t.} \quad \boldsymbol{g}(\boldsymbol{x}, \boldsymbol{y})=\boldsymbol{0} \tag{8-b}$$
$$y_i(1-y_i)=0, \quad i=1,2,\ldots,m \tag{8-c}$$
$$\boldsymbol{x}^{\min} \le \boldsymbol{x} \le \boldsymbol{x}^{\max} \tag{8-d}$$
$$f(\boldsymbol{x}, \boldsymbol{y}) \le C^d-\varepsilon \tag{8-e}$$

Step 5: Let $(\boldsymbol{x}^d, \boldsymbol{y}^d)$ denote one local optimal solution of (8). Set $C^d=f(\boldsymbol{x}^d, \boldsymbol{y}^d)$ and go back to **Step 3** until the maximum number of inner iterations is reached or the model is infeasible.

Step 6: Update C by $C=f(\boldsymbol{x}^*, \boldsymbol{y}^*)$;

Step 7: Go back to **Step 2** until the maximum number of outer iterations or infeasibility is detected.

variables, the model still takes on a nonconvex nature, and the global optimal solution is still difficult to achieve.

To address this issue, a sequential IP method in [34] is employed to solve the problem in (6), the procedure of which is shown in Table I, where ε is a small number and m denotes the number of binary variables. The procedure simply consists of two nested loops. In the outer loop, a sequence of monotonously decreasing minima of the relaxed model is obtained. In the inner loop, an attempt is made to find the best feasible minimum around every relaxed minimum obtained at the outer loop. Furthermore, the point $(\boldsymbol{x}^d, \boldsymbol{y}^d)$ leading to the best objective value is taken as the final optimal solution of the original model (2).

III. Reactive Power Optimization With Joint Transmission and Distribution Networks

A. *Hierarchical Modeling for Joint Transmission and Distribution Networks*

For the joint transmission and distribution networks, all the network buses can be divided into three types: transmission buses, distribution buses, and feeder buses, wherein the feeder buses are the boundary buses that connect distribution and transmission networks. Accordingly, the accurate reactive power optimization model for the joint transmission and distribution networks can be formulated as (9), which puts all three types of buses into one complete reactive power optimization model (2),

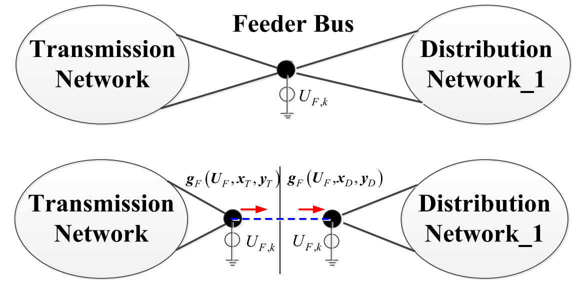

Fig. 3. Hierarchical modeling by feeder bus splitting.

$$\min \; f(\boldsymbol{x}_D, \boldsymbol{x}_T, \boldsymbol{y}_T, \boldsymbol{y}_D, \boldsymbol{U}_F) \tag{9-a}$$
$$\text{s.t.} \; \boldsymbol{g}(\boldsymbol{x}_D, \boldsymbol{x}_T, \boldsymbol{y}_T, \boldsymbol{y}_D, \boldsymbol{U}_F)=\boldsymbol{0} \tag{9-b}$$
$$\boldsymbol{x}_D^{\min} \le \boldsymbol{x}_D \le \boldsymbol{x}_D^{\max} \tag{9-c}$$
$$\boldsymbol{x}_T^{\min} \le \boldsymbol{x}_T \le \boldsymbol{x}_T^{\max} \tag{9-d}$$
$$\boldsymbol{U}_F^{\min} \le \boldsymbol{U}_F \le \boldsymbol{U}_F^{\max}. \tag{9-e}$$

In order to solve the optimization model (9) by hierarchical modeling, we take one distribution network connected to the transmission network, for example, as shown in Fig. 3. Once the voltage magnitude of the feeder bus $U_{F,k}$ is available, the entire joint network can be split into two individual networks by adding one voltage source for each splitting bus with the voltage value being as the original feeder bus $U_{F,k}$. Equivalently, (9) can be reformulated as (10) with respect to the three types of network buses, where N is the number of distribution networks

$$\min \; f_T(\boldsymbol{x}_T, \boldsymbol{y}_T, \boldsymbol{U}_F)+\sum_{k=1}^{N} f_{D,k}(\boldsymbol{x}_{D,k}, \boldsymbol{y}_{D,k}, U_{F,k}) \tag{10-a}$$
$$\text{s.t.} \; \boldsymbol{g}_T(\boldsymbol{x}_T, \boldsymbol{y}_T, \boldsymbol{U}_F)=\boldsymbol{0} \tag{10-b}$$
$$g_{F,k}(\boldsymbol{x}_T, \boldsymbol{y}_T, \boldsymbol{U}_F)=g_{F,k}(\boldsymbol{x}_{D,k}, \boldsymbol{y}_{D,k}, U_{F,k}), \quad k=1,2,..,N \tag{10-c}$$
$$\boldsymbol{g}_{D,k}(\boldsymbol{x}_{D,k}, \boldsymbol{y}_{D,k}, U_{F,k})=\boldsymbol{0}, \quad k=1,2,..,N \tag{10-d}$$
$$\boldsymbol{x}_{D,k}^{\min} \le \boldsymbol{x}_{D,k} \le \boldsymbol{x}_{D,k}^{\max}, \quad k=1,2,..,N \tag{10-e}$$
$$\boldsymbol{x}_T^{\min} \le \boldsymbol{x}_T \le \boldsymbol{x}_T^{\max} \tag{10-f}$$
$$\boldsymbol{U}_F^{\min} \le \boldsymbol{U}_F \le \boldsymbol{U}_F^{\max} \tag{10-g}$$

where the subscript D and T denote the set of buses in the distribution and transmission networks, respectively, and the subscript F denotes the set of feeder buses.

Assuming the power flow from the kth transmission network to distribution network is $\dot{S}_k$, where the dot on top of $\dot{S}_k$ denotes the complex power, we have

$$g_{F,k}(\boldsymbol{x}_T, \boldsymbol{y}_T, \boldsymbol{U}_F)=g_{F,k}(\boldsymbol{x}_{D,k}, \boldsymbol{y}_{D,k}, U_{F,k})=\dot{S}_k. \tag{11}$$

Then, the centralized modeling in (10) can be decomposed into one transmission-level optimization model and k

distribution-level optimization models such that

$$\min\ f_T\left(\boldsymbol{x}_T,\ \boldsymbol{y}_T,\ \boldsymbol{U}_F\right) \tag{12-a}$$

$$\text{s.t.}\ \boldsymbol{g}_T\left(\boldsymbol{x}_T,\ \boldsymbol{y}_T,\ \boldsymbol{U}_F\right) = \boldsymbol{0} \tag{12-b}$$

$$g_{F,k}\left(\boldsymbol{x}_T,\ \boldsymbol{y}_T,\ \boldsymbol{U}_F\right) = S_k, \quad k = 1, 2, .., N \tag{12-c}$$

$$\boldsymbol{x}_T^{\min} \le \boldsymbol{x}_T \le \boldsymbol{x}_T^{\max} \tag{12-d}$$

$$\boldsymbol{U}_F^{\min} \le \boldsymbol{U}_F \le \boldsymbol{U}_F^{\max}. \tag{12-e}$$

For the *k*th distribution network, the reactive power optimization model can be expressed as

$$\min\ f_{D,k}\left(\boldsymbol{x}_{D,k},\ \boldsymbol{y}_{D,k},\ U_{F,k}\right) \tag{13-a}$$

$$\text{s.t.}\ \boldsymbol{g}_{D,k}\left(\boldsymbol{x}_{D,k},\ \boldsymbol{y}_{D,k},\ U_{F,k}\right) = \boldsymbol{0} \tag{13-b}$$

$$g_{F,k}\left(\boldsymbol{x}_{D,k},\ \boldsymbol{y}_{D,k}, U_{F,k}\right) = \dot{S}_k \tag{13-c}$$

$$\boldsymbol{x}_{D,k}^{\min} \le \boldsymbol{x}_{D,k} \le \boldsymbol{x}_{D,k}^{\max} \tag{13-d}$$

$$U_{F,k}^{\min} \le U_{F,k} \le U_{F,k}^{\max}. \tag{13-e}$$

In the above hierarchical framework, the models in (12) and (13) can be performed separately. Specifically, the SCADA system of the transmission network only captures the information at the transmission network level by adding the use of coded signals over communication channels. Then, the EMS performs the reactive power optimization considering both transmission and feeder buses at the transmission network level. Also, the DMS only acquires the local-area information with each individual network, then performs reactive power optimization model considering both distribution and feeder buses.

B. Curve-Fitting Approach for a Decomposition Method

The feeder buses, however, are coupled in both transmission and distribution networks. Therefore, the big challenge is that the optimal solution S_k, $k = 1,..., N$, from (12) and (13), may not be consistent. This means that the minimization of transmission network losses may have conflicts with minimizing losses at each distribution network, attaining different S_k.

To force the consistent optimal solution S_k from (12) and (13), $\dot{S}_k$ in (12-c) should contain the information of the distribution networks. Fortunately, from the distribution network model in (13), it can be observed that for a given voltage magnitude of the feeder bus, the optimal solution of each distribution network S_k can be evaluated by executing the model given in (13). In this sense, the optimal solution $\dot{S}_k$ is actually a function of the feeder bus voltage magnitude such that $\dot{S}_k = h_{D,k}(U_{F,k})$. Moreover, let R_k denote the total load demand of *k*th distribution network and the total losses of *k*th distribution network are $\mathrm{real}(\dot{S}_k) - R_k$, which is the objective function of reactive optimization model in (13).

Nevertheless, the accurate closed form of the nonlinear function $h_{D,k}(\cdot)$ is generally difficult to obtain. Therefore, a curve-fitting approach is proposed to approximate the function $h_{D,k}(\cdot)$. Since $h_{D,k}(U_{F,k})$ is only related to a single variable $U_{F,k}$ with the range of $U_{F,k}^{\min} \le U_{F,k} \le U_{F,k}^{\max}$, we can discretize $U_{F,k}$ by w_k points $U_{F,k}^{(1)}$, ..., $U_{F,k}^{(i)}$, ..., $U_{F,k}^{(w_k)}$. For each voltage magnitude $U_{F,k}^{(i)}$, solving the model in (14) by a sequential IP method gives the corresponding power flow $\dot{S}_k = h_{D,k}^{(i)}(x_{F,k}^*,\ y_{F,k}^*)$, where $(x_{F,k}^*,\ y_{F,k}^*)$ is the optimal solution from

$$h_{D,k}^{(i)}\left(\boldsymbol{x}_{D,k}^*,\ \boldsymbol{y}_{D,k}^*\right) = \underset{\dot{S}_k}{\operatorname{argmin}}\ f_{D,k}\left(\boldsymbol{x}_{D,k},\ \boldsymbol{y}_{D,k},\ U_{F,k}^{(i)}\right) \tag{14-a}$$

$$\text{s.t.}\ \boldsymbol{g}_{D,k}\left(\boldsymbol{x}_{D,k},\ \boldsymbol{y}_{D,k},\ U_{F,k}^{(i)}\right) = \boldsymbol{0} \tag{14-b}$$

$$\boldsymbol{x}_{D,k}^{\min} \le \boldsymbol{x}_{D,k} \le \boldsymbol{x}_{D,k}^{\max} \tag{14-c}$$

$$x_{F,k}^{\min} \le x_{F,k} \le x_{F,k}^{\max}. \tag{14-d}$$

Furthermore, the curve-fitting approach aims to find the function $h_{D,k}(\cdot)$ that satisfies the mapping

$$\left(U_{F,k}^{(1)}, ..., U_{F,k}^{(i)}, ..., U_{F,k}^{(w_k)}\right) \xrightarrow{h_{D,k}(*)} \left(h_{D,k}^{(1)}\left(\boldsymbol{x}_{D,k}^*, \boldsymbol{y}_{D,k}^*\right), ..., h_{D,k}^{(i)}\left(\boldsymbol{x}_{D,k}^*, \boldsymbol{y}_{D,k}^*\right), ..., h_{D,k}^{(w_k)} \times \left(\boldsymbol{x}_{D,k}^*, \boldsymbol{y}_{D,k}^*\right)\right). \tag{15}$$

Thus, a curve-fitting technique [35] is employed to give an approximated "smooth" function that has the best fit to a series of data points. There are a number of methods to implement curve fitting. Here, we choose the polynomial functions and increase the degree of the polynomial equation to achieve an exact match, wherein fitting means trying to find the approximated polynomial function $\overline{h}_{D,k}(\cdot)$ that minimizes the orthogonal distance to the data points (e.g., least squares) so that

$$\min_{\overline{z}_{D,k}(*)} \sum_{k=1}^{w_k} \left(\overline{h}_{D,k}\left(U_{F,k}^{(i)}\right) - h_{D,k}^{(i)}\left(U_{F,k}\right)\right)^2. \tag{16}$$

After obtaining the approximated polynomial function $\overline{h}_{D,k}(\cdot)$, we have $\dot{S}_k \approx \overline{h}_{D,k}(U_{F,k})$.

As aforementioned, in order to guarantee the decomposition method to be equivalent to the accurate model in (13), the optimal solution S_k from the transmission network and distribution network models should be strictly consistent. To achieve that $\dot{S}_k \approx \overline{h}_{D,k}(U_{F,k})$ can be added into the transmission network model in (12), which yields

$$\min\ f_T\left(\boldsymbol{x}_T,\ \boldsymbol{y}_T,\ \boldsymbol{U}_F\right) + \sum_{k=1}^{N}\left(\mathrm{real}\left(\overline{h}_{D,k}\left(U_{F,k}\right)\right) - R_k\right) \tag{17-a}$$

$$\text{s.t.}\ \boldsymbol{g}_T\left(\boldsymbol{x}_T,\ \boldsymbol{y}_T,\ \boldsymbol{U}_F\right) = \boldsymbol{0} \tag{17-b}$$

$$g_{F,k}\left(\boldsymbol{x}_T,\ \boldsymbol{y}_T,\ \boldsymbol{U}_F\right) = \overline{h}_{D,k}\left(U_{F,k}\right), \quad k = 1, 2, .., N \tag{17-c}$$

$$\boldsymbol{x}_T^{\min} \le \boldsymbol{x}_T \le \boldsymbol{x}_T^{\max} \tag{17-d}$$

$$\boldsymbol{U}_F^{\min} \le \boldsymbol{U}_F \le \boldsymbol{U}_F^{\max}. \tag{17-e}$$

As shown in Fig. 4, it should be noted that: 1) the optimal solution $\dot{S}_k$ from the transmission network model (17) is forced to be equal to $\overline{h}_{D,k}(U_{F,k})$, which approximates to the exact value of each distribution network model (13), i.e., $h_{D,k}(U_{F,k})$, so the optimality of distribution networks can be approximately

This article has been accepted for inclusion in a future issue of this journal. Content is final as presented, with the exception of pagination.

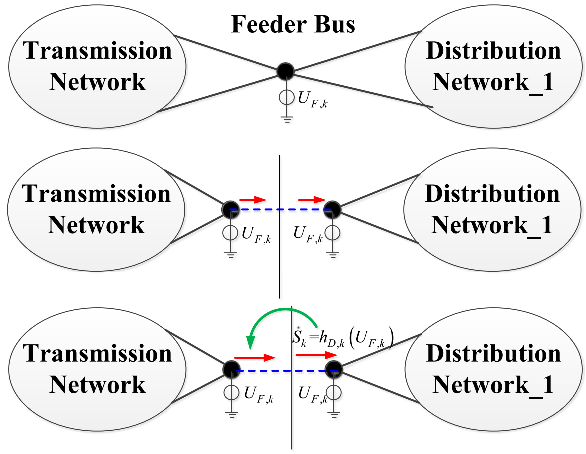

Fig. 4. Decomposition by feeder bus splitting.

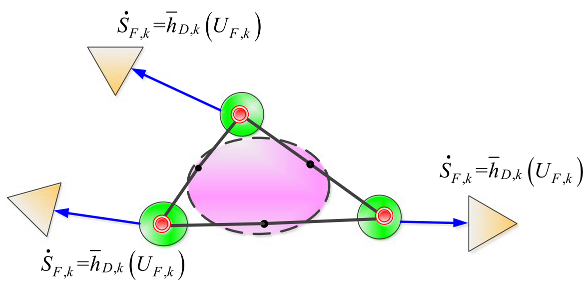

Fig. 5. Physical meaning of the CFF.

achieved; and 2) the constant number R_k in the objective function can be eliminated, which will not affect the optimal solution. Thus, the model in (17) can be reformulated as

$$\min \ f_T(\boldsymbol{x}_T, \boldsymbol{y}_T, \boldsymbol{U}_F) + \sum_{k=1}^{N} \text{real}\left(\bar{h}_{D,k}(U_{F,k})\right) \quad \text{(18-a)}$$

$$\text{s.t.} \ \boldsymbol{g}_T(\boldsymbol{U}_F, \boldsymbol{x}_T, \boldsymbol{y}_T) = \boldsymbol{0} \quad \text{(18-b)}$$

$$g_{F,k}(\boldsymbol{x}_T, \boldsymbol{y}_T, \boldsymbol{U}_F) = \bar{h}_{D,k}(U_{F,k}), \quad k = 1, 2, .., N \quad \text{(18-c)}$$

$$\boldsymbol{x}_T^{\min} \le \boldsymbol{x}_T \le \boldsymbol{x}_T^{\max} \quad \text{(18-d)}$$

$$\boldsymbol{U}_F^{\min} \le \boldsymbol{U}_F \le \boldsymbol{U}_F^{\max}. \quad \text{(18-e)}$$

It is obvious that the reactive power optimization for joint transmission and distribution networks can be decomposed by the CFF. First, (18) is performed on the transmission network level; then, the optimal solution $(\boldsymbol{x}_T^*, \boldsymbol{y}_T^*, \boldsymbol{U}_F^*)$ can be obtained by the sequential IP method. Second, after obtaining the optimal solution of the new transmission network, the optimal solution of each distribution network can be directly solved by the inverse of the CFF. Since the CFF is an approximated function, we can calculate the approximated optimal solution of each distribution network by (14) with respect to the optimal solution $U_{F,k}^*$ from (18).

Intuitively, the physical meaning of the model (18) can be illustrated in Fig. 5. For the transmission network model (10), each distribution network connected to the feeder bus can be equivalent to a CFF. Meanwhile, the objective should take into account the CFF as a cost function, such that all the distribution networks can be cooperated. Hence, this new joint network model can reflect the information of distribution networks.

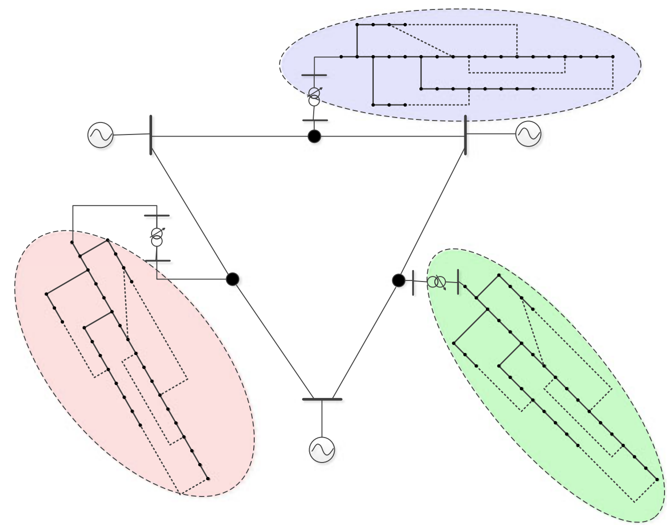

Fig. 6. Topology of the joint WSCC 9-bus transmission network and 33-bus distribution networks.

IV. Numerical Example

In this section, the proposed modeling method is tested on two test systems and the reactive power optimization is carried out by the sequential IP method on a personal computer with an Intel Core i5 Duo Processor T420 (2.50 GHz) and 4-GB RAM (32-bit system).

A. *Joint WSCC 9-Bus Transmission Network and 33-Bus Distribution Networks*

In this case, a 345-kV WSCC 9-bus transmission system in Fig. 6 is used where each load bus is connected to a 63-kV 33-bus distribution network. The topology of the distribution network is the same as the original case [36], but the load demands with both reactive and active powers are modified by scaling the base load via a factor such that the total load demands are consistent with the values given by the transmission network [37].

For the 33-bus distribution system, we assume that two switchable capacitors/reactors (SCs/SRs) are connected to buses 3 and 6 whose capacities are [−0.6, +0.6] MVar and the step sizes of the SCs/SRs are 0.3 and 0.2 MVar, respectively. As for the transmission network level, only the reactive power outputs of thermal generators are taken into account.

First, the general CFF for the three load buses is tested by using a quadratic polynomial expression such that $P_k(Q_k) = \alpha U_k^2 + \beta U_k + \gamma$. Discretizing the voltage magnitude of each feeder bus U_k within [0.9, 1.1] p.u. with the step of 0.02 p.u. is then done, and the errors are compared in Table II, where the maximum error (ME) of all buses resulting from the quadratic polynomial functions is less than 0.23%, which can be acceptable by practical power systems. Meanwhile, the CFF

TABLE II
QUADRATIC CFF FOR CENTRALIZED AND HIERARCHICAL METHODS

	CFF for active power			CFF for reactive power		
	#5	#7	#9	#5	#7	#9
α	90.29	152.70	100.65	61.19	103.80	68.01
β	−214.68	−355.47	−242.15	−145.32	−241.38	−163.47
γ	135.46	217.46	155.45	91.53	147.41	104.78
ME.	0.13%	0.15%	0.23%	0.12%	0.14%	0.23%

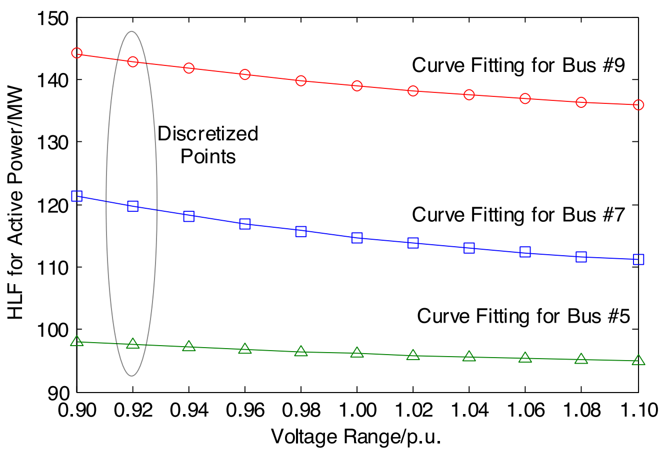

Fig. 7. CFF for the active power.

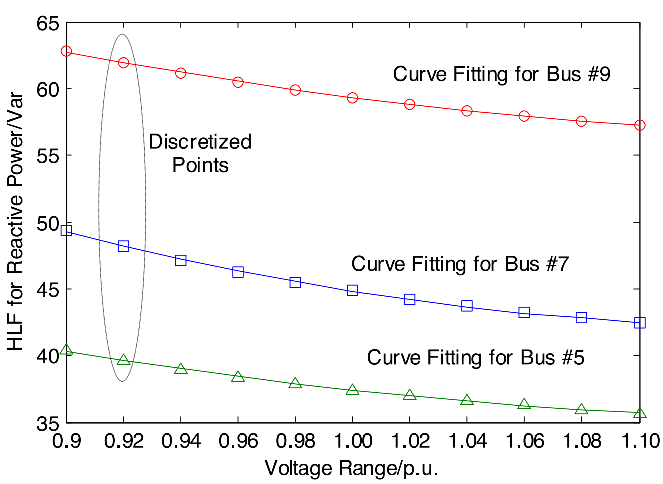

Fig. 8. CFF for the reactive power.

for active and reactive powers is plotted in Figs. 7 and 8, respectively, which implies that the CFF functions strictly decrease with the increase of the voltage magnitude. Institutively, the CFF functions include two parts: power losses and the total load demand. Since the total load demand is constant, the decreasing CFF functions with respect to the voltage magnitude also suggest that a higher voltage magnitude leads to less active and reactive power losses. Figs. 9 and 10 depict the error between centralized and hierarchical methods under different load factors. It can be observed that the error becomes larger with the increase of the load factor, but the ME will not exceed 1%.

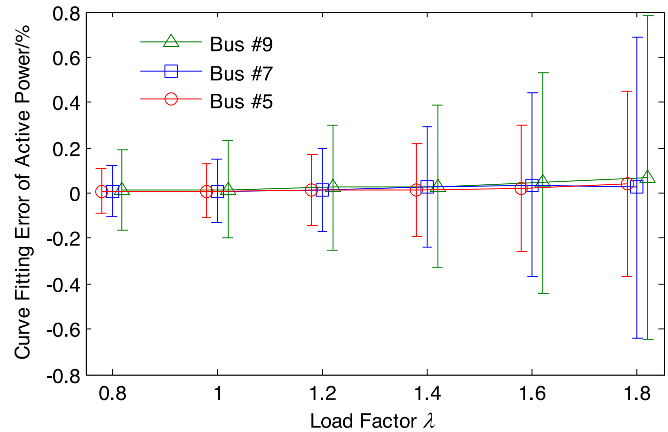

Fig. 9. Curve-fitting error for the active power.

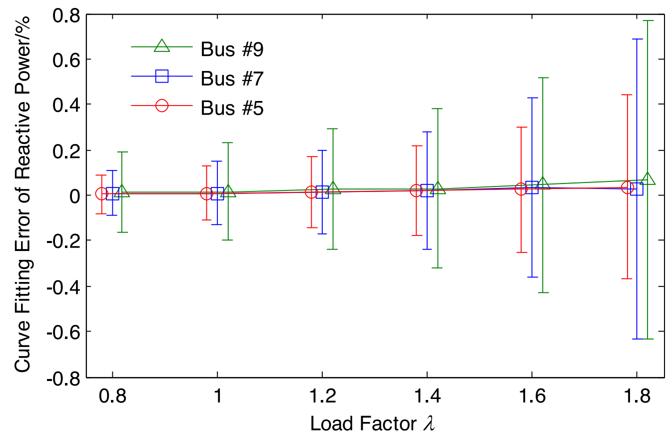

Fig. 10. Curve-fitting error using a quadratic function for the reactive power.

TABLE III
COMPARISONS OF TRANSMISSION/DISTRIBUTION NETWORK LOSSES BETWEEN CENTRALIZED AND HIERARCHICAL METHODS

Method	T.	D.-#5	D.-#7	D.-#9	Total
Normal	5.4130	16.1673	19.5517	19.5876	60.7196
Centralized	2.5301	9.7470	12.6314	12.7640	37.6725
Hierarchical	2.6232	9.7574	12.6259	12.7859	37.7924
Error	3.68%	0.11%	0.04%	0.17%	0.32%

Furthermore, the comparisons of transmission/distribution network losses between centralized and hierarchical methods are presented in Table III, where the centralized method is taken as the benchmark. At first, it can be observed that under normal conditions without reactive power optimization, the total power loss is about 60.7196 MW; the reactive power optimization can reduce 37.95% of the power loss. The ME of distribution network losses is no more than 0.17% (about 0.02 MW), the error of distribution network losses is 3.68% (about 0.09 MW), and the error of the total network losses is relatively small, i.e., 0.32% (about 0.12 MW).

The voltage magnitudes by centralized and hierarchical methods at each feeder bus are compared in Table IV. The reactive power optimization can clearly improve the voltage profile, and the comparison between the proposed and centralized methods

TABLE IV
COMPARISONS OF VOLTAGE MAGNITUDE BETWEEN CENTRALIZED AND HIERARCHICAL METHODS

Bus	#1	#2	#3	#4	#5
Normal	1.0000	1.0000	1.0000	0.9870	0.9750
Centralized	1.0600	1.0600	1.0544	1.0545	1.0439
Hierarchical	1.0600	1.0600	1.0544	1.0541	1.0435
Bus	#6	#7	#8	#9	
Normal	1.0020	0.9830	0.9950	0.9560	
Centralized	1.0600	1.0482	1.0597	1.0317	
Hierarchical	1.0600	1.0484	1.0600	1.0310	

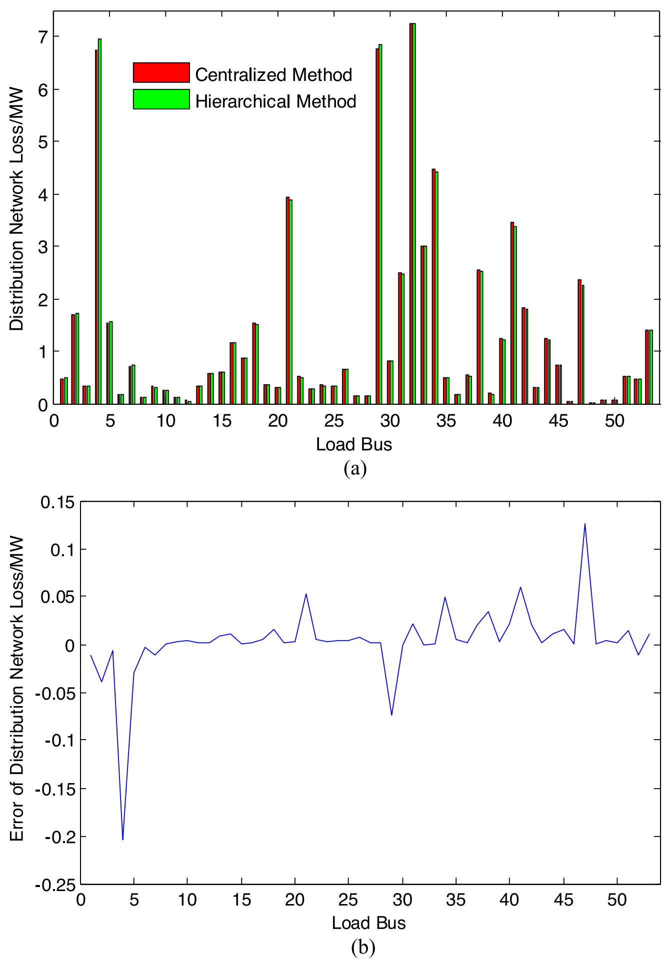

Fig. 11. Comparison of distribution network losses between centralized and hierarchical methods. (a) Distribution network loss. (b) Error of distribution network loss.

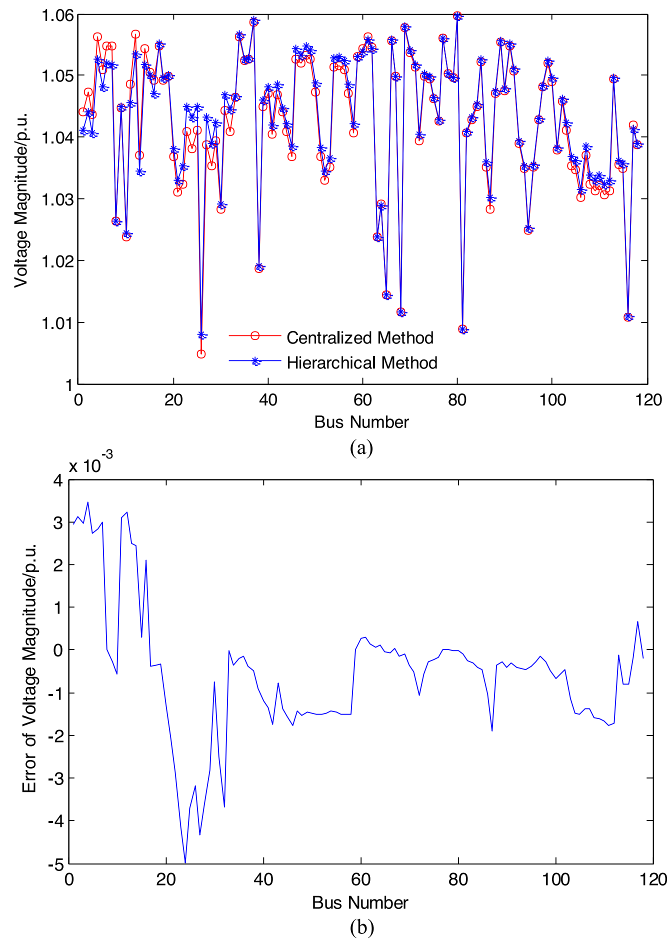

Fig. 12. Comparison of voltage magnitude between centralized and hierarchical methods. (a) Voltage magnitude. (b) Error of voltage magnitude.

suggests that the hierarchical method attains nearly the same optimization results as the benchmarked method, verifying the effectiveness of the proposed method.

B. Joint IEEE 118-Bus Transmission Network and 123-Bus Distribution Networks

In this case, a 138-kV WSCC 118-bus transmission system is utilized and each load bus is connected to a 35-kV 123-bus distribution network. The topology of the 123-bus distribution network is the same as the original case in [31], and the total load demands (a.k.a., reactive and active powers) are consistent with the values given by the transmission network [32]. Five reactive power compensators are connected to bus 12, 35, 54, 76, and 108, which can be continuously adjusted. The capacity of each continuous compensator ranges in $[-0.1, +0.1]$ MVar.

In Fig. 11, the distribution network losses using centralized and hierarchical methods are compared, in which the error of each distribution network between centralized and hierarchical methods ranges from -3.02% to 5.29%. Also, the transmission network losses calculated with the centralized and hierarchical methods are 9.15 and 9.23 MW, respectively, and the error between the two methods is about 0.87%. For the total network losses combined with transmission and distribution networks, the centralized and hierarchical methods give 76.13 and 76.38 MW, respectively, where the error between the two methods is 0.25 MW, i.e., 0.33% of the total network losses. Similarly, voltage magnitudes between the centralized and hierarchical methods are compared in Fig. 12, where the voltage magnitudes between the two methods are roughly the same and the ME is less than 0.5% and the average error is lower than 0.1%. On the whole, the results from Figs. 11 and 12 verify the effectiveness of the proposed method.

TABLE V
COMPUTATIONAL TIME FOR THE TWO TEST SYSTEMS

Test Systems	9-33-bus			118-123-bus		
Methods	Pro.		Cen.	Pro.		Cen.
# of variables	60		643	952		39753
# of constraints	63		653	1074		39874
Time (s)	Solver	CFF	Solver	Solver	CFF	Solver
	0.23	5.88	36.54	4.72	8.27	1000.72

C. Computational Performance

Finally, the compuational time of the two test systems in Sections IV-A and IV-B is presented in Table V. It illustrates that the proposed method (Pro.) outperforms the centralized method (Cen.). Specifically, in the 9-33-bus system, Pro. needs a total of only 6.11 s to solve a nonlinear programming by the traditional IPM, whereas Cen. takes 36.54 s to solve a MINLP by the sequential IP method; and in the 118-123-bus system, all the reactive power compensators are assumed to be continousely adjusted, and the reactive power optimization is solved by IPM. Pro. needs 12.99 s in total, but Cen. takes about 1000 s, which is more than 100 times slower than what Pro. does. Moreover, it can be found that computing for HLF by the repetitive solutions of the optimization problem (13) under different values of the boundary voltage is absolutely independent. That means we can solve the problem (13) under different values of the boundary voltage in a parallel framework, which will further accelerate the speed of obtaining HLF.

Thanks to the proposed CFF for each distribution network, the number of variables and constraints in the proposed hierarchical model is significantly reduced compared to the centralized model, which greatly facilitates the modeling in the control center and improves the computational time of the reactive power optimization.

V. CONCLUSION

This paper has developed a hierarchical reactive power optimization model to minimize the total network losses of joint transmission and distribution networks. Unlike the traditional centralized modeling, the hierarchical modeling performs the reactive power optimization model of transmission and distribution networks separately, alleviating big data problems for the control center. Moreover, in order to achieve the global optimality of the centralized modeling, a curve-fitting approach has been proposed to provide a cost function of the distribution network model for the transmission network model, so that all the distribution networks can be coordinated. Numerical results on two test systems show that the proposed method can efficiently deal with joint transmission and distribution network models, with the error of the optimal solution compared to the centralized method very small.

REFERENCES

[1] T. Ding, S. Liu, W. Yuan, Z. Bie, and B. Zeng, "A two-stage robust reactive power optimization considering uncertain wind power integration in active distribution networks," *IEEE Trans. Sustain. Energy*, vol. 7, no. 1, pp. 301–311, Jan. 2016.

[2] S. Corsi *et al.*, "Coordination between the reactive power scheduling function and the hierarchical voltage control of the EHV ENEL system," *IEEE Trans. Power Syst.*, vol. 10, no. 2, pp. 686–694, May 1995.

[3] T. Ding *et al.*, "A quadratic robust optimization model for automatic voltage control on wind farm side," in *Proc. IEEE Power Energy Soc. Gen. Meet.*, Vancouver, BC, Canada, 2013, pp. 1–5.

[4] W. Zhang, F. Li, and L. M. Tolbert, "Review of reactive power planning: Objectives, constraints, and algorithms," *IEEE Trans. Power Syst.*, vol. 22, no. 4, pp. 2177–2186, Nov. 2007.

[5] W. S. Jwo, C. W. Liu, C. C. Liu, and Y. T. Hsiao, "Hybrid expert system and simulated annealing approach to optimal reactive power planning," *IET Proc. Gener., Transm. Distrib.*, vol. 142, no. 4, pp. 381–385, 1995.

[6] Y. L. Chen and Y. L. Ke, "Multi-objective VAr planning for large-scale power systems using projection-based two-layer simulated annealing algorithms," *IEE Proc. Gener., Transm. Distrib.*, vol. 151, no. 4, pp. 555–560, 2004.

[7] K. Y. Lee and F. F. Yang, "Optimal reactive power planning using evolutionary algorithms: A comparative study for evolutionary programming, evolutionary strategy, genetic algorithm, and linear programming," *IEEE Trans. Power Syst.*, vol. 13, no. 1, pp. 101–108, Feb. 1998.

[8] Q. H. Wu and J. T. Ma, "Power system optimal reactive power dispatch using evolutionary programming," *IEEE Trans. Power Syst.*, vol. 10, no. 3, pp. 1243–1249, Aug. 1995.

[9] Y. Wang, F. Li, and Q. Wan, "Reactive power planning based on fuzzy clustering and multivariate linear regression," in *Proc. IEEE Power Energy Soc. Gen. Meeting*, Minneapolis, MN, USA, 2010, pp. 1–6.

[10] Y. Wang, F. Li, Q. Wan, and H. Chen, "Multi-objective reactive power planning based on fuzzy clustering and learning automata," in *Proc. Int. Conf. Power Syst. Technol.*, 2010, pp. 1–7.

[11] Y. Wang, F. Li, Q. Wan, and H. Chen, "Reactive power planning based on fuzzy clustering, gray code, and simulated annealing," *IEEE Trans. Power Syst.*, vol. 26, no. 4, pp. 2246–2255, Nov. 2011.

[12] K. Iba, "Reactive power optimization by genetic algorithm," *IEEE Trans. Power Syst.*, vol. 9, no. 2, pp. 685–692, May 1994.

[13] R. A. Gallego, A. J. Monticelli, and R. Romero, "Optimal capacitor placement in radial distribution networks," *IEEE Trans. Power Syst.*, vol. 16, no. 4, pp. 630–637, Nov. 2001.

[14] B. Zhao, C. X. Guo, and Y. J. Cao, "A multiagent-based particle swarm optimization approach for optimal reactive power dispatch," *IEEE Trans. Power Syst.*, vol. 20, no. 2, pp. 1070–1078, May 2005.

[15] H. Yoshida *et al.*, "A particle swarm optimization for reactive power and voltage control considering voltage security assessment," *IEEE Trans. Power Syst.*, vol. 15, no. 4, pp. 1232–1239, Nov. 2000.

[16] C. H. Dai, W. R. Chen, Y. F. Zhu, and X. X. Zhang, "Seeker optimization algorithm for optimal reactive power dispatch," *IEEE Trans. Power Syst.*, vol. 24, no. 3, pp. 1218–1231, Aug. 2009.

[17] K. Y. Lee, Y. M. Park, and J. L. Ortiz, "A united approach to optimal real and reactive power dispatch," *IEEE Trans. Power App. Syst.*, vol. 104, no. 5, pp. 1147–1153, May 1985.

[18] J. A. Momoh, S. X. Guo, E. C. Ogbuobiri, and R. Adapa, "The quadratic interior-point method solving power-system optimization problems," *IEEE Trans. Power Syst.*, vol. 9, no. 3, pp. 1327–1336, Aug. 1994.

[19] O. Alsac, J. Bright, M. Prais, and B. Stott, "Further developments in LP-based optimal power flow," *IEEE Trans. Power Syst.*, vol. 5, no. 3, pp. 697–711, Aug. 1990.

[20] N. Grudinin, "Reactive power optimization using successive quadratic programming method," *IEEE Trans. Power Syst.*, vol. 13, no. 4, pp. 1219–1225, Nov. 1998.

[21] D. I. Sun *et al.*, "Optimal power flow by Newton approach," *IEEE Trans. Power App. Syst.*, vol. PAS-103, no. 10, pp. 2864–2880, Oct. 1984.

[22] M. B. Liu, S. K. Tso, and Y. Cheng, "An extended nonlinear primal-dual interior-point algorithm for reactive-power optimization of large-scale power systems with discrete control variables," *IEEE Trans. Power Syst.*, vol. 17, no. 4, pp. 982–991, Nov. 2002.

[23] K. Aoki, M. Fan, and A. Nishikori, "Optimal var planning by approximation method for recursive mixed-integer linear-programming," *IEEE Trans. Power Syst.*, vol. 3, no. 4, pp. 1741–1747, Nov. 1988.

[24] N. Deeb and S. M. Shahidehpour, "Linear reactive power optimization in a large power network using the decomposition approach," *IEEE Trans. Power Syst.*, vol. 5, no. 2, pp. 428–478, May 1990.

[25] T. Ding *et al.*, "A robust two-level coordinated static voltage security region for centrally integrated wind farms," *IEEE Trans. Smart Grid*, vol. 7, no. 1, pp. 460–470, Jan. 2016.

[26] H. Sun *et al.*, "A two-level distributed approach to power network modeling," *IEEE Trans. Power Del.*, vol. 30, no. 3, pp. 1496–1504, Jun. 2015.

[27] Z. Li, Q. Guo, H. Sun, and J. Wang "A new LMP-sensitivity-based heterogeneous decomposition for transmission and distribution coordinated economic dispatch," *IEEE Trans. Smart Grid*, to be published.

[28] Z. Li, Q. Guo, H. Sun, and J. Wang, "Coordinated economic dispatch of coupled transmission and distribution systems using heterogeneous decomposition," *IEEE Trans. Power Syst.*, vol. 31, no. 6, pp. 4817–4830, Nov. 2016.

[29] Z. Li, Q. Guo, H. Sun, and J. Wang, "Coordinated transmission and distribution AC optimal power flow," *IEEE Trans. Smart Grid*, to be published.

[30] C. Lin, W. Wu, B. Zhang, B. Wang, W. Zheng, and Z. Li, "Decentralized reactive power optimization method for transmission and distribution networks accommodating large-scale DG integration," *IEEE Trans. Sustain. Energy*, vol. 8, no. 1, pp. 363–3730, Jan. 2017.

[31] P. Aristidou and T. V. Cutsem, "Dynamic simulations of combined transmission and distribution systems using decomposition and localization," in *Proc. IEEE Power Tech Conf.*, Grenoble, France, 2013, pp. 1–6.

[32] D. C. Little *et al.*, "An algorithm for the traveling salesman problem," *Oper. Res.*, vol. 11, no. 6, pp. 972–989, 1963.

[33] G. Cornuejols, "Valid inequalities for mixed integer linear programs," *Math. Prog. Ser. B*, vol. 112, pp. 3–44, 2008.

[34] J. R. Santos *et al.*, "Finding improved local minima of power system optimization problems by interior-point methods," *IEEE Trans. Power Syst.*, vol. 18, no. 1, pp. 238–244, Feb. 2003.

[35] M. K. William, *Curve Fitting for Programmable Calculators*. Syntec, Inc., Winthrop Harbor, WA, USA, 1984.

[36] R. D. Zimmerman, C. E. Murillo-Sánchez, and R. J. Thomas, "MATPOWER: Steady-state operations, planning, and analysis tools for power systems research and education," *IEEE Trans. Power Syst.*, vol. 26, no. 1, pp. 12–19, Feb. 2011.

[37] (2014). [Online]. Available: http://shgl.curent.utk.edu/toolsdemo/

Tao Ding (S'13–M'15) received the B.S.E.E. and M.S.E.E. degrees from Southeast University, Nanjing, China, in 2009 and 2012, respectively, and the Ph.D. degree from Tsinghua University, Beijing, China, in 2015.

During 2013–2014, he was a Visiting Scholar with the Department of Electrical Engineering and Computer Science, The University of Tennessee, Knoxville, TN, USA. He is currently an Associate Professor with the State Key Laboratory of Electrical Insulation and Power Equipment, School of Electrical Engineering, Xi'an Jiaotong University, Xi'an, China. He has authored or co-authored more than 60 technical papers and was published by "Springer Theses" recognizing outstanding Ph.D. research around the world and across the physical sciences—*Power System Operation With Large Scale Stochastic Wind Power Integration*. His current research interests include electricity markets, power system economics and optimization methods, and power system planning and reliability evaluation.

Dr. Ding was the recipient of the Excellent Master and Doctoral Dissertation from Southeast University and Tsinghua University, respectively, and the Outstanding Graduate Award of Beijing City.

Cheng Li (S'16) received the B.S. degree from the School of Electrical Engineering, Xi'an Jiaotong University, Xi'an, China, in 2016, where he is currently working toward the M.S. degree.

His major research interests include power system optimization and renewable energy integration.

Can Huang (GS'13–M'16) received the B.S.E.E degree from Hohai University, Nanjing, China, in 2008, the M.S.E.E. degree from Southeast University, Nanjing, in 2011, and the Ph.D. degree from The University of Tennessee, Knoxville, TN, USA, in 2016.

From 2011 to 2012, he was with the State Grid Electric Power Research Institute (NARI Group Corporation), Nanjing. He is currently a Postdoctoral Research Staff Member with the Lawrence Livermore National Laboratory, Livermore, CA, USA. His current research interests include advanced control, computing, and communication for power and energy systems.

Yongheng Yang (S'12–M'15) received the B.Eng. degree from Northwestern Polytechnical University, Xi'an, China, in 2009, the Postgraduate degree from Southeast University, Nanjing, China, in 2011, and the Ph.D. degree from Aalborg University, Aalborg, Denmark, in 2014.

In 2013, he was a Visiting Scholar with Texas A&M University. Since 2014, he has been with the Department of Energy Technology, Aalborg University, where he is currently an Assistant Professor. His research interests include grid integration of renewable energy systems, power converter design, analysis and control, harmonics identification and mitigation, and reliability in power electronics. He has authored or co-authored more than 80 technical papers and coauthored *Periodic Control of Power Electronic Converters* (IET, 2017).

Dr. Yang is a member of the IEEE Power Electronics Society (PELS) Students and Young Professionals Committee, where he serves as the Global Strategy Chair and is responsible for the IEEE PELS Students and Young Professionals Activities. He served as a Guest Associate Editor of the IEEE JOURNAL OF EMERGING AND SELECTED TOPICS IN POWER ELECTRONICS, and has also been invited as a Guest Editor of *Applied Sciences*. He is an active reviewer for a number of journals.

Fangxing Li (M'01–SM'05–F'17) received the B.S.E.E. and M.S.E.E. degrees from Southeast University, Nanjing, China, in 1994 and 1997, respectively, and the Ph.D. degree from the Virginia Polytechnic Institute and State University, Blacksburg, VA, USA, in 2001.

He was with ABB Consulting as a Senior Engineer and then a Principal Engineer from 2001 to 2005. He is currently a Professor with The University of Tennessee, Knoxville, TN, USA. His current research interests include renewable energy integration, power markets, distributed energy resources, and smart grid.

Dr. Li is a Registered Professional Engineer in the State of North Carolina, an Editor of the IEEE TRANSACTIONS ON SUSTAINABLE ENERGY, an Editor of IEEE POWER ENGINEERING LETTERS, and the Vice-Chair of the PSOPE Committee.

Frede Blaabjerg (S'86–M'88–SM'97–F'03) received the Ph.D. degree from Aalborg University, Aalborg, Denmark, in 1992.

He was with ABB-Scandia, Randers, Denmark, from 1987 to 1988. He became an Assistant Professor in 1992, an Associate Professor in 1996, and a Full Professor of power electronics and drives in 1998 with Aalborg University. His current research interests include power electronics and its applications such as in wind turbines, PV systems, reliability, harmonics, and adjustable speed drives.

Prof. Blaabjerg was the recipient of 17 IEEE Prize Paper Awards, the IEEE Power Electronics Society Distinguished Service Award in 2009, the EPE-PEMC Council Award in 2010, the IEEE William E. Newell Power Electronics Award in 2014, and the Villum Kann Rasmussen Research Award in 2014. He was an Editor-in-Chief of the IEEE TRANSACTIONS ON POWER ELECTRONICS from 2006 to 2012. He was nominated by Thomson Reuters as one of the most 250 cited researchers in Engineering in the world in 2014 and 2015, respectively.